

New Developments in Defect Studies in Semiconductors

L. C. Kimerling

Bell Laboratories
Murray Hill, New Jersey

A survey of the agenda of this conference over the past ten years indicates a decline in interest in the fundamental properties of defects in semiconductors. This trend is in accordance with the more pragmatic approaches to device and systems development in evidence today. For instance, there is little one can do to prevent displacement damage in a hostile environment. For a given solid and energetic radiation, a specific displacement cross section is inevitable. However, related point defect phenomena, which were once buried in the noise of semiconductor device behavior, are now limiting yield, performance, and reliability. High energy radiation provides a convenient means for the clean and controlled introduction of point defects. A renewed interest has, therefore, been stimulated in order to develop an understanding of the basic limitations of solid state materials and materials processing in use today. The purpose of this work is to report significant new results in defect studies and indicate the impact of these ideas on today's problems.

Experimental

In semiconductors, the study of defect states located within the forbidden gap provides a background free means for observation of the presence and properties of defects. The techniques on which we base this report, capacitance transient spectroscopy and scanning electron microscope (SEM) charge collection microscopy, employ essentially a device structure, a p-n junction or Schottky barrier, and measure defect properties as changes in the device response to external excitation. Most of the results to be reported relate to point defect behavior observed by capacitance transient spectroscopy. However, the scanning electron microscope techniques are critical to the study of line and planar defects and will be discussed briefly.

Junction capacitance techniques have been employed in the study of the electronic states of point defects for over ten years.^{1,2} Electronic transitions corresponding to the charging and discharging of defect states within the depletion region may be studied by observation of associated changes in the junction capacitance. Because each defect state possesses a unique energy position and capture cross section, the junction response to thermal or optical excitation reveals selectively the electronic transitions at each defect. The recent introduction of junction bias pulsing techniques by Lang³ has created a spectroscopic tool for observation of defect states. A defect spectrum may be generated by repetitive pulsing of the junction bias from a fixed reverse voltage toward forward bias. Defect states

which are filled during the pulse may empty during the period between pulses if sufficient thermal energy is present to stimulate a bound to band transition. The resultant capacitance transient may be analyzed through signal processing instrumentation that is tuned to a specific recovery rate. As the sample temperature is scanned from the dopant freeze out region to higher temperatures, a peak in the signal processor output is observed when the decay rate of the capacitance transient is coincident with the instrumental rate window. The activation energy for carrier emission from a defect state to a band represents the approximate energy position of the defect state and can be derived from the temperature dependence of the emission rate or the change in the temperature at which a peak is observed with a corresponding change in rate window. Capture processes are observed directly by monitoring a decrease in the peak signal as the pulse width (or filling time) is reduced. Lang³ employed a double boxcar instrument as a rate discriminator. Miller⁴ has since introduced an optimized exponential correlator for the same purpose. Kimerling⁵ has modified the basic technique for use in a calibrated system with commercially available instrumentation. A schematic of the system, which uses a lock-in amplifier to set the rate window, is shown in Fig. 1.

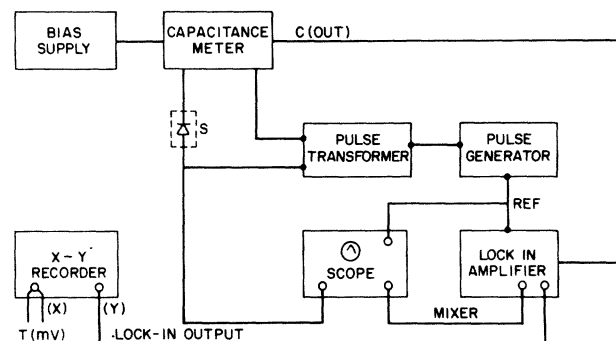


Fig. 1 Simplified capacitance transient spectroscopy system for use in the study of the electrical properties of point defects.

SEM charge collection microscopy allows the separation of line and planar defects from a point defect background. The electron beam acts as a micron sized probe which delineates the action of defects as recombination centers. A typical measurement structure which utilizes a Schottky barrier to generate the charge collection field is depicted in Fig. 2. De Kock, et al.⁶ have used the technique to study microdefects and impurity striations in dislocation-free, float-zoned silicon. A review of the princi-

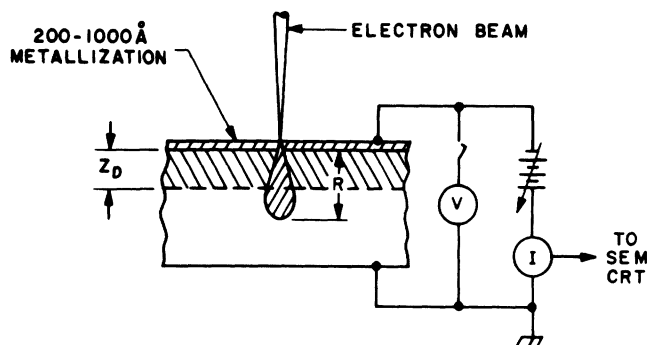


Fig. 2 Schottky diode structure as used in SEM charge collection microscopy observations of the electrical behavior of line and planar defects.

ples and applications of the measurement has been given by Leamy et al. X-ray topography and transmission electron microscopy (TEM) complement this technique with structural analysis.

In general, Schottky barrier structures are preferred for both electrical measurements because sample fabrication is simpler and non-destructive. The same sample may be used for capacitance and charge collection studies yielding a virtually complete characterization of all electrically active defects.

Silicon-Point Defects

The electrical properties of displacement damage in silicon have been studied extensively by capacitance transient spectroscopy. No conflicts, where applicable, were found with the basic results of earlier reports^{8,9}, although relative defect concentrations were strongly sample dependent. Figures 3 and 4 show typical spectra observed in n- and p-type material, respectively. (Negative signals are obtained using injection pulses and represent minority carrier emission to the minority carrier band). The behavior of a particular defect state under various bombardment particle energies and masses, background impurity contents, and annealing temperatures, provides valuable insight concerning defect identification.

Figures 5 and 6 show isochronal annealing data obtained following 1-MeV electron bombardment at room temperature. It should be emphasized that 10-MeV irradiation was used to produce the representative spectra of Figs. 3 and 4 because a more balanced distribution of defect concentrations is obtained. In n-type material the two dominant defects observed are E (0.18 eV) and H (0.42 eV). The defects are introduced at approximately the same rate and anneal together. The E (0.18 eV) state has been correlated with the A-center (vacancy-oxygen complex) which should account for most of the vacancy production in this crucible-grown material. The H (0.42 eV) state, being of equal importance, is, then, either a deeper state of the A-center or an interstitial related defect. The fact that H (0.42 eV) is observed prominently in low oxygen, float-zoned material suggests that the latter explanation may be correct. Thus, the A-center may anneal as a result of annihilation by mobile interstitial type defects. It should be mentioned here that standard diffusion techniques introduce enough oxygen into float-zoned material to make it

virtually indistinguishable from crucible grown material in these experiments. Schottky barrier structures together with photoinjection, therefore, were used in the study of the H (0.42 eV) state in the float-zoned materials.

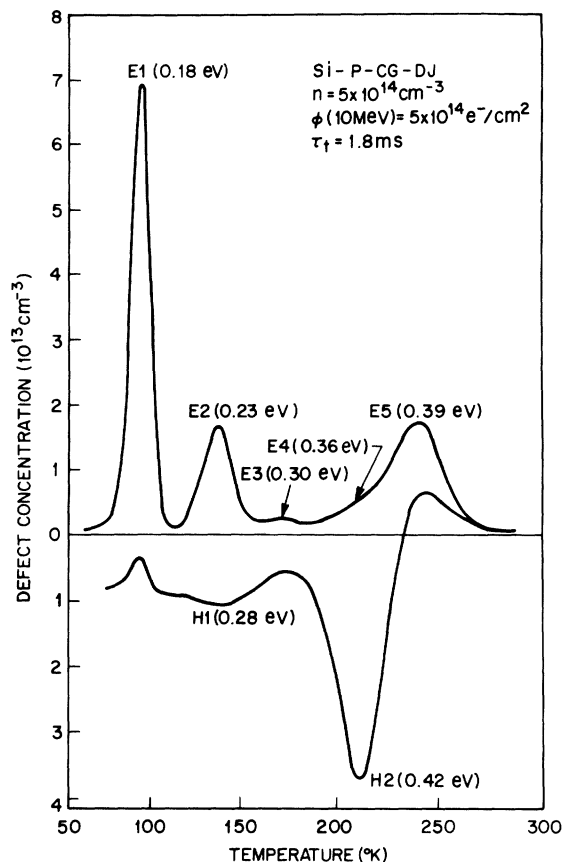


Fig. 3 Typical defect spectrum following electron irradiation of crucible grown, n-type silicon at 300°K. τ indicates the rate window employed.

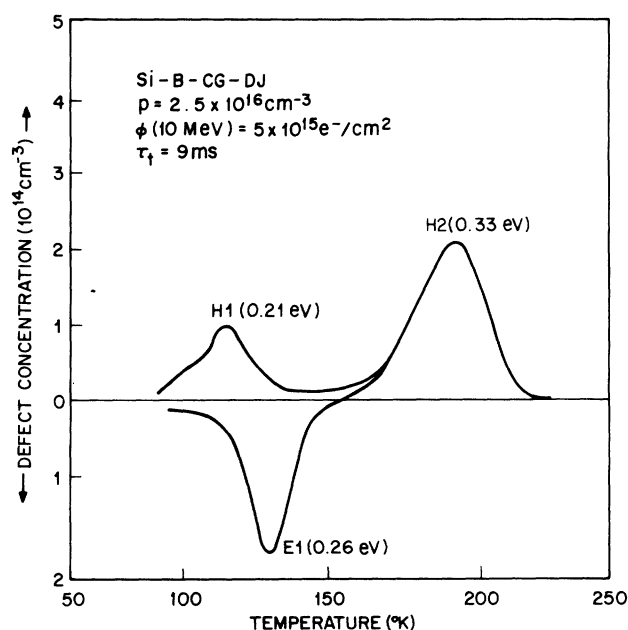


Fig. 4 Typical defect spectrum observed in crucible grown, boron-doped, p-type silicon following electron irradiation at 300°K.

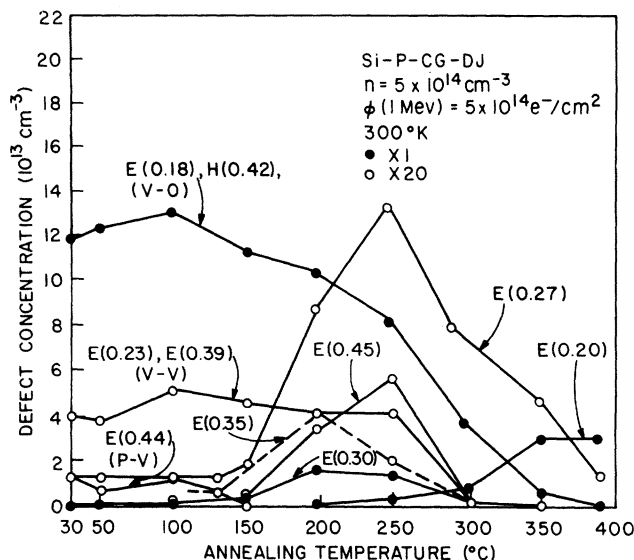


Fig. 5 Isochronal annealing (20 min.) of defects states in n-type silicon. Note that open circle data points have been multiplied by 20 times.

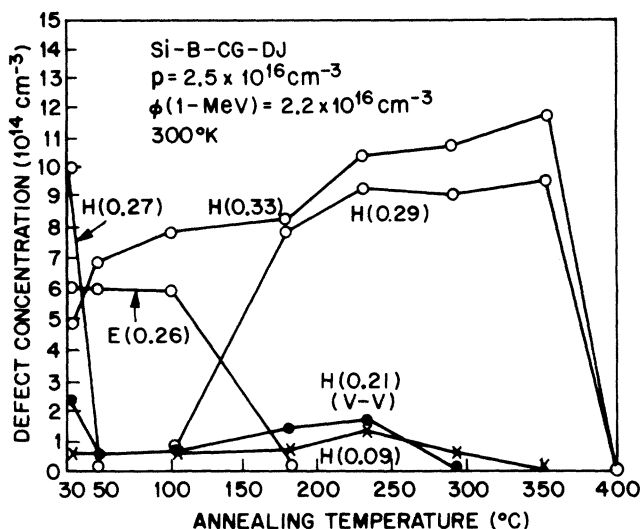


Fig. 6 Isochronal annealing (20 min.) of defect states in boron-doped, p-type silicon.

Figure 7 illustrates the particle and energy dependence of defect introduction in n-type material. It is remarkable that point defect character predominates even for alpha-particle bombardment. The E (0.39 eV) state has been correlated with the divacancy defect. The spectra in Fig. 7 have been normalized to the A-center E (0.18 eV) concentration to show the increasing importance of divacancy defects with the heavier or more energetic particles. The slight broadening of the deep peaks observed in the alpha-particle spectrum indicates the broadening of defect states because of short range electronic interactions in a local region of high defect concentration (displacement cascade). Carbon and nitrogen implantation damage have been observed to produce more severe broadening. A detailed study of defect introduction rates as a function of electron bombardment energy has been performed for both n- and p-type materials.^{10,11}

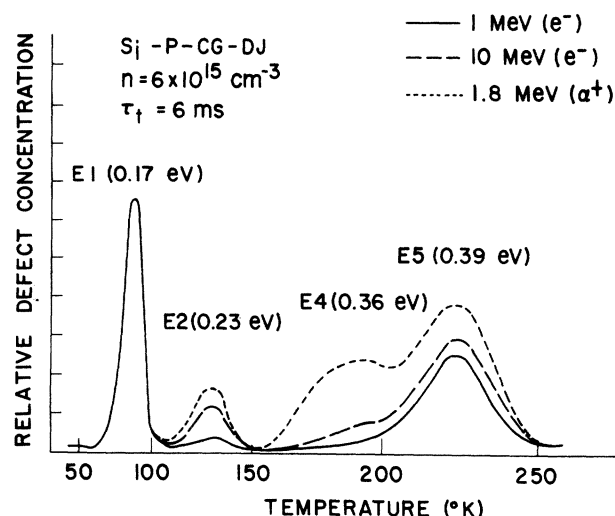


Fig. 7 Comparison of particle dependence of defect state introduction in n-type silicon. The spectra are normalized to the E1 (A-center) concentration.

Figures 8 and 9 summarize our silicon results based on comparison of capacitance transient spectroscopy studies with published electron paramagnetic resonance studies.^{12,13} The direct comparison of EPR data with the capacitance results is at times not valid, because the EPR measurements are frequently done in a high defect concentration regime while capacitance measurements always relate to dilute defect concentrations.

SILICON				
V	O-V	V-V	C ₁	C ₁ -C _s
$\sigma_n = 0.09$ OUT 90°K $\sigma_n = 10^{-14} \text{ cm}^2$ $E_a = 1.3 \text{ eV}$ $\nu = 10^8 \text{ sec}^{-1}$	$\sigma_n = 0.18$ OUT 350°K $\sigma_n = 2 \times 10^{-16} \text{ cm}^2$ $E_a = 1.3 \text{ eV}$ $\nu = 10^8 \text{ sec}^{-1}$	$\sigma_n = 0.23$ OUT 300°K $\sigma_n = 4 \times 10^{-15} \text{ cm}^2$ $\sigma_p = 2 \times 10^{-16} \text{ cm}^2$ OUT 300°K $\sigma_p = 7 \times 10^{-18} \text{ cm}^2$ OUT 300°K $\sigma_p = 8 \times 10^{-17} \text{ cm}^2$ IN 300°K OUT 400°K	$\sigma_p = 5 \times 10^{-17} \text{ cm}^2$ OUT 150°K $\sigma_p = 0.11$	$\sigma_p = 0.33$ OUT 300°K $\sigma_p = 0.27$ OUT 300°K $\sigma_p = 0.21$ OUT 300°K
+		+	+	+

Fig. 8 Background related defects observed by capacitance transient spectroscopy in irradiated silicon.

SILICON			
P-V	Al-V	Al ₁	Al ₁ -Al _s
$E_a = 1.25 \text{ eV}$ $\nu = 10^{10}$ OUT 150°K $\sigma_p = 0.44$ $\sigma_p \gg 10^{-16} \text{ cm}^2$ $E_a = 0.95 \text{ eV}$ $\nu = 10^8 \text{ sec}^{-1}$	$\sigma_p = 0.48$ OUT 200°K $\sigma_p = 7 \times 10^{-18} \text{ cm}^2$ OUT 200°K $\sigma_p = 0.25$ OUT 200°K	$\sigma_p = 0.23$ IN 200°K OUT 250°K	$\sigma_p = 0.23 \text{ eV}$ OUT 250°K
+	+	++	

Fig. 9 Impurity related defects observed by capacitance transient spectroscopy in irradiated silicon.

III-V Compounds - Point Defects

Capacitance transient spectroscopy studies have been applied to the GaAs,¹⁴ GaAlAs¹⁵ and GaP¹⁶ systems. Table I lists the defect states and introduction rates observed in GaAs and GaP following 1-MeV electron bombardment at room temperature. Defect identification is, at present, indirect in the absence of specific identifications by other techniques. There is little evidence of the role of impurities suggesting that primary defects are being observed. The orientation dependence of defect introduction in GaAs suggests that all of the room temperature stable defects are related to Ga site displacements.¹⁷ The relative change in defect energy position with Al content as Al is added to GaAs shows that the E (0.41 eV) state is tied to the valence band while all other states follow the conduction band.¹⁵ This result suggests that the E (0.41) eV state could be a vacancy-type defect composed of perturbed valence bonds.

Table I

DEFECT STATES OBSERVED AFTER 1-MeV ELECTRON BOMBARDMENT AT 300°K

n-GaAs		n-GaP	
emission energy (eV)	introduction rate (cm ⁻¹)	emission energy (eV)	introduction rate (cm ⁻¹)
E (0.08)	1.8	E (0.14)	
E (0.18)	2.8	E (0.23)	0.12
E (0.41)	0.7	E (0.32)	0.14
E (0.71)	0.08	E (0.48)	0.1
E (0.90)	0.1	E (0.62)	0.07
H (0.29)	0.7	E (0.74)	0.07
H (0.41)	*		
H (0.71)	*		

* present before irradiation E refers to conduction band,

H refers to valence band.

As the scope of studies in the compound semiconductors is broadened, correlations and identifications should be forthcoming. A word of caution, however: concepts from the elemental materials such as silicon cannot be simply transferred. Because two interpenetrating lattices are involved, simple vacancy diffusion becomes a complicated multi-jump process. The structure of defects such as the divacancy must be reconsidered.

Line and Planar Defects

SEM charge collection techniques were employed to study large defect structures present in dislocation free, float-zoned silicon (Fig. 10).⁶ Microdefects observed as recombination centers were subsequently examined by transmission electron microscopy³¹ and found to consist of interstitial type dislocation loops.³¹ At this time the results suggest that these defects represent collapsed clusters of silicon interstitials present in equilibrium at the growth temperature. The electrical activity of these defects could be totally quenched by crystal growth in an Ar-10% H₂ atmosphere. This result is an additional example of the electrical activity of hydrogen in semiconductor systems.³⁰ It is thought that hydrogen can satisfy "dangling" defect bonds, thus annihilating their activity as recombination sites.

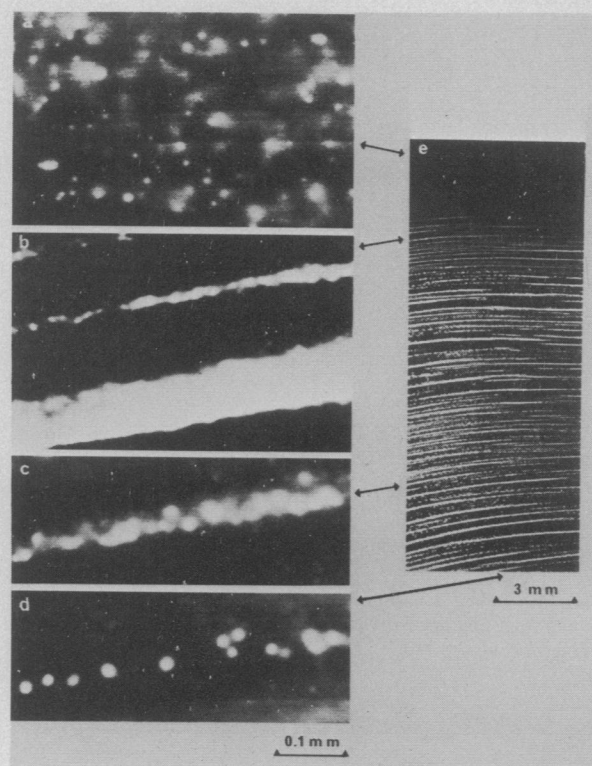


Fig. 10 Comparison of x-ray topograph following Cu decoration (e) with SEM charge collection micrographs of undecorated materials (a,b,c,d) showing growth defects in high-purity, dislocation-free, float-zoned silicon. A transition in defect structures is noted between fast (a) and slow (c,d) growth rate conditions.

Electronically Stimulated Defect Processes

Defect interactions in semiconductors are unique in that a confluence of electronic processes can influence the kinetics of simple thermally activated processes. Electric fields may be internally or externally generated. The Fermi level and, hence, defect charge states change with temperature. The band gap represents an energy reservoir which may be tapped by electronic transitions at a defect. A schematic representation of possible ionization related phenomena is shown in Fig. 11. In this section the role and magnitude of these effects in defect interaction processes will be discussed.

ELECTRONIC ENHANCEMENT MECHANISMS

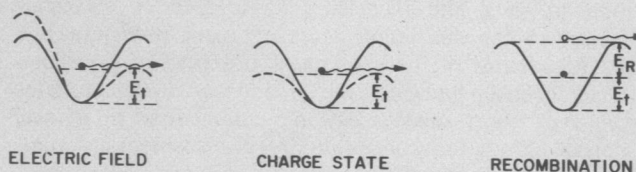


Fig. 11 Mechanisms for electronic enhancement of defect reactions.

The drift motion of point defects in an electric field has been discussed with respect to impurities¹⁸ and lattice defects¹⁹ in response to externally applied fields, and defect interactions involving internally generated fields.²⁰ The electric field acts only on charged defects and biases the direction of defect motion along the field lines. The microscopic saddle point barrier is lowered slightly by an amount $qV a/X$ where a is the distance between saddle points and X is the distance over which the potential V is applied. If one considers the process of migration out of a drift volume, the reaction enhancement factor relative to the pure thermal process is given by

$$\frac{R_E}{R_T} = \frac{qV}{kT} \quad (1)$$

where R_E is the rate of the field enhanced process, R_T is the rate of the pure thermal process, and T is the temperature. For example, a negatively-charged divacancy in silicon moving under a 100 V applied reverse bias at 600°K (a typical annealing temperature) would exhibit an enhancement factor of about 2000 for diffusion from the depletion region.

Charge State Effects

A change in the occupation of a localized defect orbital may cause a change in a reaction saddle point of the defect as the surrounding bonds relax. Evidence for such effects in low temperature vacancy migration was reported by Watkins.²¹ Kimerling et al.²² have recently found conclusive evidence for charge state effects in the annealing of the E-center (phosphorus-vacancy complex) in silicon at 150° C. Charge state changes may be stimulated by changes in the Fermi level due to temperature changes, doping changes, the introduction of compensating defect states, or the generation of a depletion region. Quasi-Fermi level changes as a consequence of minority carrier injection also modify the average charge state.

The effect is related entirely to the time spent in a specific charge state and is not dependent on a charge state fluctuation rate. The maximum enhancement effect possible for pure thermal excitation is related to the thermal energy required to change the charge state. This fact exists because as the defect attempts to surmount a large reaction barrier, it will find conditions more favorable to change charge state and pass over a smaller barrier so that the isolated effect of the barrier is not observed. Thus

$$\frac{R_{CS}}{R_T} \approx \exp \left[\frac{E_D - E_F}{kT} \right] \text{ or } \exp \left[\frac{\Delta E_T}{kT} \right] \quad (2)$$

(whichever is smaller)

where ΔE_T is the difference in the thermal reaction barriers for the two charge states and $E_D - E_F$ is the difference in energy between the defect energy level and the Fermi level. The constraint of Eq. (2) usually limits charge state effects to rather small observed enhancement factors ($< 10^3$).

Bourgoin and Corbett²³ have discussed a fluctuation rate dependent charge state process which is related to the

occurrence of a 180° phase change in the equilibrium saddle point configuration as the charge state changes. This proposal is a novel idea for an athermal diffusion process, but apparently has no isolated application in systems studied to date.²⁴

Recombination Enhanced Defect Reactions

This process is by far the most effective mode of electronic stimulation which has been observed. The mechanism was first isolated in GaAs^{25,26} by noting a faster annealing rate of defect states produced by 1-MeV electron damage when the device was under forward bias. Subsequent application of capacitance transient analyses to the study yielded a direct correlation between the recombination rate and the enhanced annealing rates. In addition, the activation energy for the pure thermal process was reduced by an amount equivalent to the electronic transition energy. Charge state and Bourgoin type processes were excluded when no enhancement was observed following excitation of only one (the lower energy) electronic transition which changed the defect charge state but involved small amounts of recombination energy. The general phenomenology of the experimental observations is shown in Fig. 12. The enhancement of the annealing reaction rate arises from the local deposition of vibrational energy as a result of a non-radiative electronic transition at the defect. Lang and Henry²⁷ have found that recombination kinetics at defect states in GaAs and GaP are suggestive of such non-radiative, phonon deposition processes.

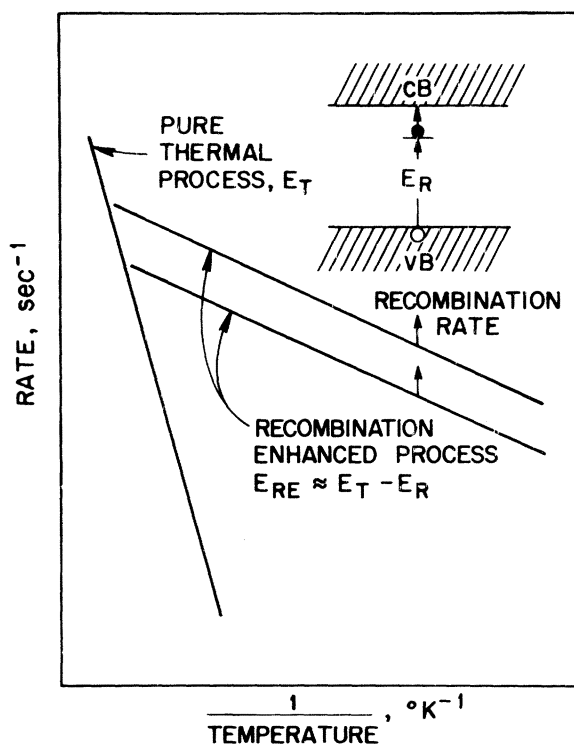


Fig. 12 Schematic of observed manifestation of recombination enhanced defect annealing. The observed activation energy (slope) is lowered by energy deposited by an electronic transition and the absolute rate (magnitude) is proportional to the recombination rate.

Weeks, Tully and Kimerling²⁸ have formulated a theoretical framework for the study of recombination enhanced processes. For a simple limiting case, $E_T > E_R$, the enhanced reaction rate may be written as

$$R_{RE} \approx \eta R_R \exp \left[-\frac{E_T - E_R}{kT} \right] \quad (3)$$

where η is an efficiency factor, R_R is the recombination rate through the defect state, E_T is the pure thermal reaction barrier, and E_R is the recombination energy deposited by the electronic transition. In this case the electronic energy supplements the thermal energy already residing at the defect. The physics behind η is complex, but it essentially describes the probability that the energy deposited at the defect is directed along the reaction coordinate. A value of η derived in GaAs for the E (0.41 eV) defect was approximately 10^{-3} . When $E_R \gg E_T$, the reaction should be athermal and Eq. (3) simplifies to

$$R_{RE} \approx \eta R_R \quad (4)$$

Both regimes have been observed in GaAs and GaP. Table II shows observed thermal (E_T) and enhanced ($E_T - E_R$) reaction barriers in comparison with the energy of the controlling electronic transition. The WTK approach holds in all cases in confirmation of the basic model. The observed enhancement factor in the $E_T > E_R$ regime may be written as

$$\frac{R_{RE}}{R_T} = \frac{R_R \eta}{\nu} \exp \left[\frac{E_R}{kT} \right] \quad (5)$$

where ν is the vibrational attempt frequency. Enhancement factors larger than 10^6 at room temperature have been observed in GaAs and athermal process (infinite enhancement) have been documented in GaP.

Table II

ANNEALING OF DEFECTS IN n-GaAs AND n-GaP			
Defect	Activation Energy of Thermal Anneal	Hole Transition Energy	Activation Energy of Injection Anneal
GaAs			
E (0.18)	1.75 eV (500°K)	1.2 eV	0.98 eV (425°K)
E (0.41)	1.4 eV (475°K)	1.09 eV	0.34 eV (350°K)
GaP			
E (0.14)	1.7 eV (500°K)	2.15 eV	athermal
E (0.23)	1.3 eV (450°K)	2.1 eV	athermal
E (0.32)	1.3 eV (450°K)	2.0 eV	athermal
E (0.48)	1.7 eV (500°K)	1.8 eV	athermal
E (0.62)	1.3 eV (450°K)	0.62 eV*	0.62 eV (400°K)
E (0.74)	2.1 eV (530°K)	1.5 eV	0.83 eV (400°K)

*electron transition energy

Two criteria must be met in a defect system for recombination enhancement to be an important process: 1) strong electron-phonon coupling at the defect and 2) large electronic transition energies. It is probable that the ionicity of compound materials plays a role in the coupling of electronic to vibrational energy. It is obvious that large band gap materials can provide larger electronic energies. An extreme case is the radiolysis of alkali halide materials

in which atomic displacement processes are generated by electronic transitions.

Recombination enhanced processes have not been observed in silicon above room temperature. Injection stimulated defect annealing of the E-center defect has been observed, but the kinetics cannot be distinguished from the previously discussed charge state effects. The relatively small band gap of silicon is probably the dominant factor. Inserting reasonable values of $R_R = 10^7 \text{ sec}^{-1}$, $\eta = 10^{-3}$, and $\nu = 10^{13} \text{ sec}^{-1}$, E_R must be greater than 0.6 eV for significant enhancement to be observed at 300°K and larger for higher temperatures. It is experimentally not possible to increase R_R at a defect in an unlimited fashion as sample heating and recombination shunt paths become active. At low temperatures, for low reaction barriers, photoexcitation and injection effects have been observed^{29,30} and are currently under study.

Low Temperature Impurity Diffusion

Interest in ionization enhanced diffusion processes was stimulated by reports of long range impurity migration observed in silicon at low temperatures under the influence of ionizing radiation.³² Subsequent experiments have not been able to confirm these results in all cases.³³ Kimerling and Uggerhoj³⁴ have extensively investigated the Au-Si system using both as-deposited and alloyed Au¹⁹⁸ radiotracers. No enhancement effect was observed employing white light, 1.15 μm monochromatic light, 20 keV or 50 keV electrons, 30 kV X-rays or He-Ne laser excitation.

It is doubtful that an effect will be present even if impurity mobility can be stimulated. For instance, if Au solubility in silicon decreases to insignificant levels at room temperature (as is true for Cu), the diffusion into the solid is not limited by kinetics but rather by the lack of a strong gradient in chemical potential. Thus the impurity atom would prefer to stay in the metallic surface phase. High solubility impurities such as lithium would be better suited for such studies. However, high solubility infers weak perturbation to the host lattice and, hence, a minimal configurational interaction with electronic carriers. A more effective approach would be to quench in a supersaturated concentration of a deep center impurity. The ionization of an electron beam in a TEM could be used for in situ studies of ionization stimulated precipitation processes.

The question arises concerning just how prevalent ionization effects are in everyday defect phenomena. Firstly, from the considerations of the previous section, reactions cannot be driven by fluctuations about equilibrium at very low temperatures. External excitation in the form of thermal or electronic energy must be introduced. The Bourgoin mechanism is subject to these same constraints, that is, the external energy supplied must exceed the reactive barrier if athermal behavior is to be observed. Secondly, variation in thermally stimulated reaction kinetics from sample to sample may signal that the reaction is controlled by thermally stimulated electronic transitions rather than the acquisition of kinetic energy from the heat bath.

The apparent low temperature migration of the silicon interstitial (4.2°K) has been a prime source for speculation concerning ionization enhanced processes.²⁴ Watkins³⁶ and Brower³⁷ have discussed impurity-interstitial structures observed in silicon by EPR techniques. Their results suggest a <100> split configuration for the Si interstitial in

silicon. However, for $(C)_I$ in Si this configuration requires a 0.88 eV activation and temperatures of the order of 300°K before motion is observed. Brower³⁷ has suggested that since mass transfer is not required for the motion of $(Si)_I$, the activation energy for motion could be reduced. An alternative approach is the concept of an extended interstitial disturbance rather than a point defect. An impurity may serve to condense the interstitial disturbance at a lattice site. In the absence of an impurity, a unique site for the interstitial may be inherently unstable. Entropy is maximized and enthalpy is minimized if the point defect relaxes to a longer range disturbance which minimizes the effects of unsatisfied or distorted bonds. In this configuration, defect motion would be equivalent to propagation of an acoustic wave. If the structure exists, an interstitial wavelet could very well exhibit low temperature motion without the benefit of enhancement processes.

High Temperature Impurity Diffusion

The diffusion of phosphorus in silicon exhibits an anomalous profile. Initially, the phosphorus concentration drops off faster than an error function would predict, and then an extended tail region of apparent enhanced diffusivity is observed. Beyond the diffusion front, buried layer regions exhibit enhanced diffusion (emitter dip effect) indicating the propagation of diffusion related defects from the phosphorus containing region.

The poor control over the broadened profile has resulted in the use of As rather than P diffusion in narrow base devices. Diffusion of As exhibits a very steep profile characteristic of the initial region of the P diffusion, and subsequent tail and emitter dip effects are minimal. Peart and Newman³⁸ first suggested that breakup of E-center defects by Fermi level controlled charge state effects²² could produce excess vacancies which would act to enhance both phosphorus and buried layer diffusion beyond the region of breakup. This approach has been attacked on the grounds that As should behave similarly.

Gilmer and Kimerling³⁹ have considered the equilibrium between the diffusing entities (PV) , $(PV)^-$, $(V)^0$, $(V)^-$, $(P)^+$, and electrons and holes in the system. A first principles calculation was made based on defect data derived from displacement damage studies. Figure 13 shows the results of numerical calculations which imply that under equilibrium conditions the fraction of mobile phosphorus will decrease with decreasing phosphorus concentration and hence, the diffusion coefficient will display a strong concentration dependence. This effect arises from the fact that the diffusing $(P)^+$ controls the Fermi level. As $(P)^+$ decreases along the profile, $(V)^-$, $(PV)^-$, and (PV) decrease. At high $(P)^+$ mobile phosphorus is essentially all $(PV)^-$. As $(P)^+$ decreases, the fraction of mobile phosphorus shows an n^2 dependence reflecting the two electrons captured by the negative E-center. At low $(P)^+$ concentrations, there is a cross over point as the Fermi level passes through the E-center defect level. The negative defect $(PV)^-$ becomes neutral $(PV)^0$ and its binding energy is reduced,²² and free vacancies may be liberated. If equilibrium is strictly maintained, Fig. 13 should accurately reflect the diffusion profiles. Thus a natural break in the diffusion profile should occur when all vacancies are neutral and the vacancy concentration ceases to be a function of $(P)^+$. In this case the diffusion constant should

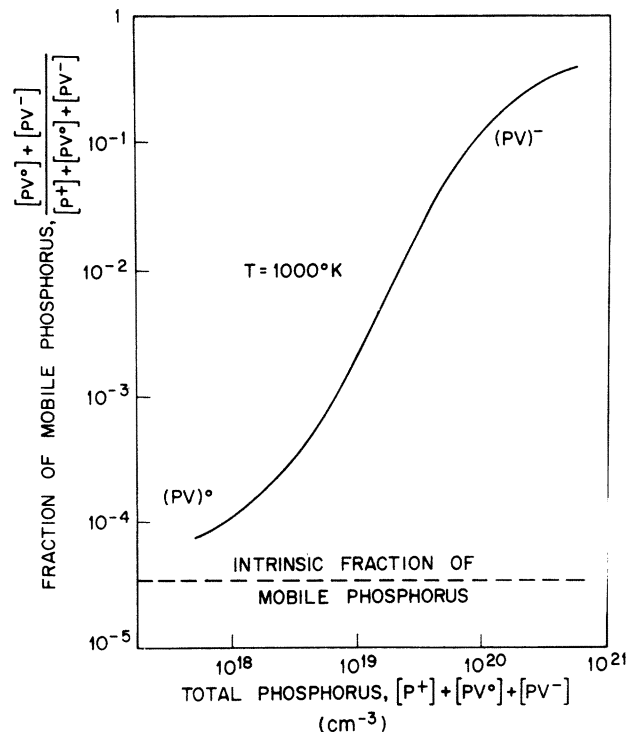


Fig. 13 Equilibrium fraction of mobile phosphorus (paired with a vacancy) as a function of total phosphorus concentration within a phosphorus diffusion profile in silicon at 1000°K.

tend toward concentration independence.

The vacancy concentration before the charge state cross over is at equilibrium with the phosphorus which has "carried" it in from the surface. Beyond the cross over, the equilibrium total vacancy concentration is low because $(P)^+$ is low. When the charge state change occurs, the cross over point acts as a buried source of excess vacancies. A steady state vacancy flux is generated from this region to the crystal surfaces in an effort to restore equilibrium. The effect of this vacancy flow is greatest in the tail region of the profile where the fraction of mobile phosphorus is lowest.

Fair and Tsai⁴⁰ have approached the problem independently, by analysis of actual diffusion profiles. Their results and model parameters are fully consistent with the first principle approach. The treatment is remarkably thorough and demonstrates that emitter dip behavior follows the model closely. The contrast between arsenic and phosphorus behavior is explained in terms of differences in the prefactor of the Arrhenius relation for the diffusion coefficient.

Device Reliability

Injection mode semiconductor devices, particularly those constructed from III-V compound materials, display a well known tendency to degrade while in operation. Essentially all semiconductor devices are based on non-equilibrium junction structures. If injection conditions acted universally to stimulate defect mobility, then, under operation, kinetic barriers would be removed and the device structure would tend to homogenize itself in an act of self destruction. This thought strikes horror in the minds of those depending on solid state lasers in the development of a reliable optical communications system.

The fact that tunnel diodes, light emitting diodes and lasers all tend to degrade, only under operation, suggests strongly that minority carrier interactions are involved in the degradation process. Gold and Weisberg⁴¹ proposed that recombination events could produce atomic displacements in GaAs tunnel diodes and produce defects which were responsible for degradation. This idea has not yet been confirmed. Typical displacement energies are 10-15 eV while typical band gaps are 1-2 eV. We have subjected GaAs to extreme injection levels with micron sized, kilovolt electron beams at near microamp current levels and no defect introduction was observed.⁴² It is possible, however, that impurities which at equilibrium occupy both interstitial and substitutional lattice positions (such as the transition metals in Si) could be moved with less energy.⁴¹ No such impurity related phenomena have been reported.

As discussed previously, recombination enhanced defect motion has been observed. Thus, defects which meet the criteria²⁸ will be mobile within the active region of the device. We have shown that recombination enhanced defect motion can promote dislocation climb at room temperature in GaAs heterostructures.⁴² A feasible mechanism has, therefore, been established for the dark-line-defect mode of degradation in which a dislocation network, which quenches lasing action, grows in the active region during device operation. Upon closer study, Petroff and Kimerling⁴³ have concluded that, even though climb is a two site process, observed climb configurations in GaAs and GaP (grown by liquid phase epitaxy) can result from a supersaturation of a single type of interstitial defect. During the climb process, complementary vacancies on the other site are produced. As an example, a supersaturation of Ga interstitials (Ga_i) can produce dislocation climb leaving behind an excess of As vacancies (As_v).



The thermodynamic driving force for the reaction would be the larger formation energy of $(Ga)_i$. The picture which emerges from these preliminary findings is that defects incorporated in the device structure during growth become mobile under device operation, and take part in the formation of non radiative, optically dead regions in the device. Recent results of Ertenberg et al. suggesting that band gap,⁴⁴ growth rate,⁴⁵ and stoichiometry⁴⁶ are important to device lifetime, reflect consistency with the above ideas.

Electronically stimulated defect processes are not always deleterious. Barnes, for instance, has noted that injection conditions can increase the radiation tolerance of GaAs LED's⁴⁷ and lasers.⁴⁸ The ability to electronically anneal defects by selective addressing of devices has wide ranging applications such as in the programming of logic arrays.⁴⁹

In conclusion, reliability testing cannot be done by simple thermal aging. Electronic stress must also be applied. It is also conceivable that Fermi level changes upon heating could make Arrhenius type extrapolations invalid. For better or for worse electronically stimulated processes are active and important in all semiconductors. In long-lived applications such as solid state lasers and solar cells, these effects must be critically evaluated.

Acknowledgment

The assistances of J. L. Benton in sample preparation is acknowledged. The high energy electron irradiations were performed at the AFCRL Linac facility with the cooperation of H. M. DeAngelis and L. F. Lowe.

- [1] C. T. Sah and V. G. K. Reddi, IEEE Trans. Electron Devices ED-11, 345 (1964).
- [2] C. T. Sah, L. Forbes, L. L. Rosier and A. F. Tasch, Jr., Solid St. Electron. 13, 759 (1970).
- [3] D. V. Lang, J. Appl. Phys. 45, 3023 (1974).
- [4] G. L. Miller, J. V. Ramirez and D. A. H. Robinson, J. Appl. Phys. 46, 2638 (1975).
- [5] L. C. Kimerling, 1974, unpublished.
- [6] A. J. R. de Kock, S. D. Ferris, L. C. Kimerling, and H. J. Leamy, Appl. Phys. Lett. 27, 313 (1975).
- [7] H. J. Leamy, L. C. Kimerling and S. D. Ferris, Scanning Electron Microscopy/1976 (Part IV) (IIT Research Institute, Chicago, 1976) p. 529.
- [8] J. W. Walker and C. T. Sah, Phys. Rev. B7, 4587 (1973).
- [9] H. M. DeAngelis, J. W. Diebold and L. C. Kimerling, Radiation Damage and Defects in Semiconductors (Institute of Physics, London, 1973), p. 295.
- [10] L. C. Kimerling, Bull. Am. Phys. Soc. 21, 296 (1976).
- [11] L. C. Kimerling, Int. Conf. on Radiation Effects in Semiconductors, Dubrovnik 1976.
- [12] G. D. Watkins, Defects in Solids V2, edited by J. H. Crawford, Jr. and L. M. Slifkin (Plenum, New York, 1975) p. 333.
- [13] G. D. Watkins and K. L. Brower, to be published.
- [14] D. V. Lang and L. C. Kimerling, Lattice Defects in Semiconductors 1974 (Institute of Physics, London, 1975), p. 581.
- [15] D. V. Lang, R. A. Logan and L. C. Kimerling, Int. Conf. on Physics of Semiconductors, Rome, 1976.
- [16] D. V. Lang and L. C. Kimerling, Appl. Phys. Lett. 28, 248 (1976).
- [17] D. V. Lang, R. A. Logan and L. C. Kimerling, to be published.
- [18] E. M. Pell, Phys. Rev. 119, 1222 (1960); J. Appl. Phys. 32, 1048 (1961).
- [19] P. Baruch, J. Appl. Phys. 32, 653 (1961).
- [20] L. C. Kimerling and P. J. Drevinsky, IEEE Trans. Nucl. Sci. NS-18, 60 (1971).
- [21] G. D. Watkins, Symposium on Radiation Effects in Semiconductor Components (Journies d'Electronique, Toulouse) Vol. 1, p. 1.
- [21] L. C. Kimerling, H. M. DeAngelis and J. W. Diebold, Solid St. Comm. 16, 171 (1975).
- [23] J. C. Bourgoin and J. W. Corbett, Phys. Lett. 38A, 135 (1972).

- [24] J. C. Bourgoin and J. W. Corbett, *Lattice Defects in Semiconductors 1974*, (Institute of Physics, London, 1975) p. 149.
- [25] D. V. Lang and L. C. Kimerling, *Phys. Rev. Lett.* 33, 489 (1974).
- [26] L. C. Kimerling and D. V. Lang, *Lattice Defects in Semiconductors 1974*, (Institute of Physics, London, 1975) P. 589.
- [27] D. V. Lang and C. H. Henry, *Phys. Rev. Lett.* 35, 1525 (1975).
- [28] J. D. Weeks, J. C. Tully and L. C. Kimerling, *Phys. Rev. B* 12, 3286 (1975).
- [29] G. D. Watkins, *Phys. Rev. B* 12, 5824 (1975).
- [30] L. C. Kimerling and J. M. Poate, *Lattice Defects in Semiconductors 1974* (Institute of Physics, London, 1975), p. 126.
- [31] P. M. Petroff and A. J. R. de Kock, *J. Crystal Growth* 30, 117 (1975).
- [32] A. I. Koifman and O. R. Niyazova, *Phys. Stat. Solidi A* 3, K93 (1970); *Sov. Phys. Solid St.* 12, 1760 (1971).
- [33] R. S. Malkovich and I. V. Nistinyuk, *Sov. Phys. Solid St.* 16, 2082 (1975).
- [34] L. C. Kimerling and E. Uggerhoj, 1973, unpublished.
- [35] L. C. Kimerling, H. M. DeAngelis and C. P. Carnes, *Phys. Rev. B* 3, 427 (1971).
- [36] G. D. Watkins, *Bull. Am. Phys. Soc.* 21, 364 (1976).
- [37] K. L. Brower, *Bull. Am. Phys. Soc.* 21, 364 (1976).
- [38] R. F. Peart and R. C. Newman, *Radiation Damage and Defects in Semiconductors* (Institute of Physics, London, 1973) p. 170.
- [39] G. H. Gilmer and L. C. Kimerling, 1974, unpublished.
- [40] R. B. Fair and J. C. C. Tsai, to be published.
- [41] R. D. Gold and L. R. Weissberg, *Solid State Electron.* 7, 811 (1964).
- [42] L. C. Kimerling, P. M. Petroff and H. J. Leamy, *Appl. Phys. Lett.* 28, 297 (1976).
- [43] P. M. Petroff and L. C. Kimerling, *Appl. Phys. Lett.*, to be published.
- [44] M. Ettenberg and C. J. Neuse, *J. Appl. Phys.* 46, 2137 (1975).
- [45] M. Ettenberg and H. Kressel, *Appl. Phys. Lett.* 26, 478 (1975).
- [46] M. Ettenberg, G. H. Olsen and C. J. Neuse, *AIME Electronic Materials Conference*, Salt Lake City, 1976.
- [47] C. E. Barnes, *IEEE Trans. Nucl. Sci.* NS-18, 322 (1971).
- [48] C. E. Barnes, *Phys. Rev. B* 1, 4735 (1970); *J. Appl. Phys.* 45, 3485 (1974).
- [49] H. J. Leamy and L. C. Kimerling, to be published.